

Impact of Climate Change on the Density Altitude of Nine Chinese Airports

Ting Xu*

College of Aviation Meteorology, Civil Aviation Flight University of China, Deyang, 618307, China

*Corresponding Author.

Abstract:

The development of civil aviation has an impact on global climate change, and climate change will also affect the operation of civil aviation. In civil aviation, density altitude is a physical quantity used to measure aircraft performance. The higher the density altitude, the worse the aircraft performance and control efficiency. In the present work, ERA-Interim data and the output of 18 global climate models in CMIP6 were used to investigate the impact of climate change on the density altitude of nine airports in China. Historical data show that during the period 1979–2014 the density altitude of these nine airports exhibited an increasing trend, and most increased faster in spring and summer. Kace-1.0-G is the best model to simulate the historical trend of 18 global climate models, and is better than the multi-model ensemble. Using the output results of the Kace-1.0-G model under three different scenarios (SSP2-4.5, SSP3-7.0, and SSP4-8.5), the future projection of the density altitude of the nine Chinese airports in question was studied. Results show that the density altitudes of all nine airports exhibit an increasing trend from 2015 to 2100, and the higher the emission scenario, the greater the increase. Nonetheless, the model predicts that density altitude at most airports will increase faster in the winter, unlike under historical conditions.

Keywords: *Climate change, Civil aviation, Density altitude, Airport.*

I. INTRODUCTION

Climate change has become an important research topic in recent decades. Aviation activities rely on fossil fuels, the emissions from which have an impact on the climate. The 1999 report of the Intergovernmental Panel on Climate Change addresses the role of aviation activities in climate change and quantifies its contribution [1]. Considerable research has been carried out on the mechanism and quantitative estimation of aviation-induced climate change [2-6].

However, in addition to contributing to climate change, aviation activities are also expected to be negatively affected by it. For example, rising sea levels will threaten low-elevation coastal airports [7], and there will be changes in the track and intensity of storms [8-10]. Precipitation from storms will also impact airport operations. Moreover, global warming is projected to increase the frequency and intensity of extreme heat events, which will degrade aircraft performance and lead to an increase in weight restrictions

[11]. As global climate change progresses, the frequency and intensity of clear sky turbulence is also projected to increase [12-16], which poses a threat to flight safety. In addition to the impact on aviation activities, meteorological conditions also affect aircraft performance [17]. Specifically, global warming is anticipated to reduce the maximum take-off total weight [18] and increase the takeoff distance while reducing the climb rate [19].

Several physical quantities are used to measure aircraft performance, including maximum take-off total weight, takeoff distance, climb rate, and density altitude. The density altitude is the altitude relative to standard atmospheric conditions at which the air density would be equal to the indicated air density at the place of observation. A lower actual atmospheric density results in a higher density altitude and worse aircraft performance [20]. For example, the altitude of Beijing Capital International Airport is 35.3 m, and when the density height is 200 m, the aircraft performance on the ground (e.g., lift generated by the wings, engine efficiency, and other metrics) is the same as that at 200 m. Density altitude is related to physical quantities such as air temperature and air pressure and thus can be expected to be affected by climate change.

Climate models are important tools that are used to study future climate change. The Coupled Model Intercomparison Project (CMIP) was initiated in 1995 and its latest iteration, CMIP6, contains model comparison sub-programs organized and designed by experts from all over the world [21]. Scenario MIP is one of the most important of these sub-programs. On the basis of the anthropogenic emissions and land use changes generated by the energy structure that may occur in different shared socioeconomic pathways (SSPs), a new scenario prediction experiment with different combinations of SSP and radiative forcing was designed to predict the future global climate under different emission scenarios and different policy measures [22]. Therefore, in this study we used Scenario MIP to explore the climate impacts on density altitude.

II. MATERIALS AND METHODS

China represents a vast territory and complex terrain. A total of 248 civil airports are distributed on different terrains such as plains, plateaus, and basins. In order to study the density altitude characteristics of different terrains, we selected nine major airports in mainland China as the research objects (TABLE I).

TABLE I. General information for the nine airports

Name	Latitude (°N)	Longitude (°E)	Airport elevation (m)
Lhasa	29.30	90.91	3569.5
Urumqi	43.91	87.48	647.9
Xi'an	34.45	108.75	479.1
Beijing	40.07	116.60	35.3
Shanghai	31.20	121.34	3.0
Guangzhou	23.39	113.31	15.2
Shenyang	41.64	123.49	60.5

Chengdu	30.58	103.95	512.4
Qinghai	36.53	102.04	2184.2

2.1 Data

In this study, we used 18 earth system models in CMIP6 (Table II, <https://esgf-node.llnl.gov/projects/cmip6/>) to simulate the monthly data of near-surface air temperature and surface air pressure. The density altitude was then calculated based on these data according to the method described in Section 2.2. The model evaluation time period was 1979–2014, and the simulation time period was 2015–2100. The scenario models used in the future period were SSP2-4.5 (moderate development), SSP3-7.0 (localized development), and SSP4-8.5 (normal development), in which the projected radiative forcing can reach $4.5 \text{ W}\cdot\text{m}^{-2}$, $7.0 \text{ W}\cdot\text{m}^{-2}$ and $8.5 \text{ W}\cdot\text{m}^{-2}$ in 2100, respectively.

TABLE II. Basic information of the 18 earth climate system models in CMIP6

Name	Country/Region	Institution	Resolution (latitude × longitude)
ACCESS-CM2	Australia	CSIRO-ARCCSS	$1.25^\circ \times 1.875^\circ$
AWI-CM 1.1 MR	Germany	AWI	$0.93^\circ \times 0.94^\circ$
BCC-CSM2-MR	China	BCC	$1.12^\circ \times 1.12^\circ$
CAMS-CSM1-0	China	CAMS	$1.12^\circ \times 1.12^\circ$
CESM2-WACCM	United States	NCAR	$0.9^\circ \times 1.25^\circ$
CESM2	United States	NCAR	$0.9^\circ \times 1.25^\circ$
CanESM5	Canada	CCCma	$2.77^\circ \times 2.81^\circ$
EC-Earth3-Veg	EU	EC-Earth-Cons	$0.7^\circ \times 0.7^\circ$
EC-Earth3	EU	EC-Earth-Cons	$0.7^\circ \times 0.7^\circ$
FGOALS-f3-L	China	CAS	$1^\circ \times 1.25^\circ$
GFDL-ESM4	United States	NOAA-GFDL	$1^\circ \times 1.25^\circ$
INM-CM4-8	Russian	INM	$1.5^\circ \times 2^\circ$
IPSL-CM6A-LR	France	IPSL	$1.27^\circ \times 2.5^\circ$
KACE-1.0-G	Korean	NIMS-KMA	$1.25^\circ \times 1.875^\circ$
MIROC6	Japan	MIROC	$1.4^\circ \times 1.4^\circ$
MPI-ESM1.2-LR	Germany	MPI-M	$1.875^\circ \times 1.875^\circ$
MRI-ESM2.0	Japan	MRI	$1.12^\circ \times 1.12^\circ$
NorESM2-LM	Norway	NCC	$1.25^\circ \times 1.875^\circ$

ERA-Interim data were used for comparison. Monthly data of near-surface air temperature and surface air pressure from 1979 to 2014 were selected to maintain consistency with the historical simulation time of the model. The horizontal resolution was $0.7^\circ \times 0.7^\circ$.

2.2 Methods

The density altitude is not a directly measurable physical quantity. There are several methods to calculate the density altitude. In this study, it was calculated as follows:

$$DA \approx \frac{T_{SL}}{\gamma} \left[1 - \left(\frac{P/P_{SL}}{T/T_{SL}} \right)^{\left(\frac{gM}{\gamma R} - 1 \right)^{-1}} \right] \quad (1)$$

Where P is the pressure at a certain altitude, the surface air pressure was used in this study; T is the air temperature at this altitude; P_{SL} and T_{SL} are the air pressure and air temperature at sea level in the standard atmosphere, which are 1013.25 hPa and 288.15 K, respectively; γ is the vertical lapse rate of air temperature in the standard atmosphere (0.0065 K/m); g is the gravitational acceleration in the standard atmosphere (9.80665 m/s²); M is the average molecular weight in the standard atmosphere (0.028964 kg/mol); and R is 8.3144598.

The bilinear interpolation method was used in the calculation of the density altitude using the CMIP6 data and the ERA-Interim reanalysis data to interpolate the data to the latitude and longitude of each airport. The model's ability to simulate the time-dependent variation of the density altitudes of the nine airports was evaluated by analyzing the correlation coefficient, standard deviation, and root mean square error for the CMIP6 model data and the ERA-Interim data. The changes of future density altitude of the nine selected airports with different models were then compared.

III. RESULTS

3.1 Historical Changes in Density Altitude and Simulation Capability of the Cmp6 Model

TABLE III presents the mean and standard deviation of density altitudes for the nine airports in ERA-Interim. The density altitudes of the nine airports are not comparable because of the altitude difference of these airports. Except for Shenyang Airport, the average density altitudes of all airports were higher than the airport elevations, and the difference was greater for airports located in the plateau area. Thus, the aircraft performance was worse than the expected performance based on the design. In the plateau area, the aircraft performance was poor because of the low air density at high altitude, and the density altitude changes caused by changes in meteorological elements can further affect aircraft performance. The density altitudes of Shenyang, Beijing, and Urumqi airports in northern China had a large standard deviation, which is related to the large annual and inter-annual variations in air temperature and pressure. In terms of annual variation, the density altitude was highest in July and lowest in January, which is consistent with the variation in temperature.

TABLE III. Average density altitude for the nine airports based on ERA-Interim data

Airport	Lhasa	Urumqi	Xi'an	Beijing	Shanghai	Guangzhou	Shenyang	Chengdu	Qinghai
Airport elevation (m)	3569.5	647.9	479.1	35.3	3.0	15.2	60.5	512.4	2184.2
Average density altitude (m)	5104.2	1239.8	1017.5	229.8	13.0	406.5	-71.0	1036.4	3104.1
Standard deviation (m)	182.5	451.5	374.6	484.9	377.2	257.1	537.1	305.3	282.6

The density altitudes of the nine airports based on the ERA-Interim data showed a significant increasing trend (Fig 1), but the rate of increase varied among airports. Shanghai Airport and Beijing Airport had the highest rates of 2.337 and 1.786 m/a, respectively. The rate of increase of the two high-altitude airports was relatively small. The seasonal density altitude was then calculated considering the annual change of density altitude. Except for the two airports located on the plateau, all other airports showed a rapid increase in density altitude in spring and autumn (figure not included).

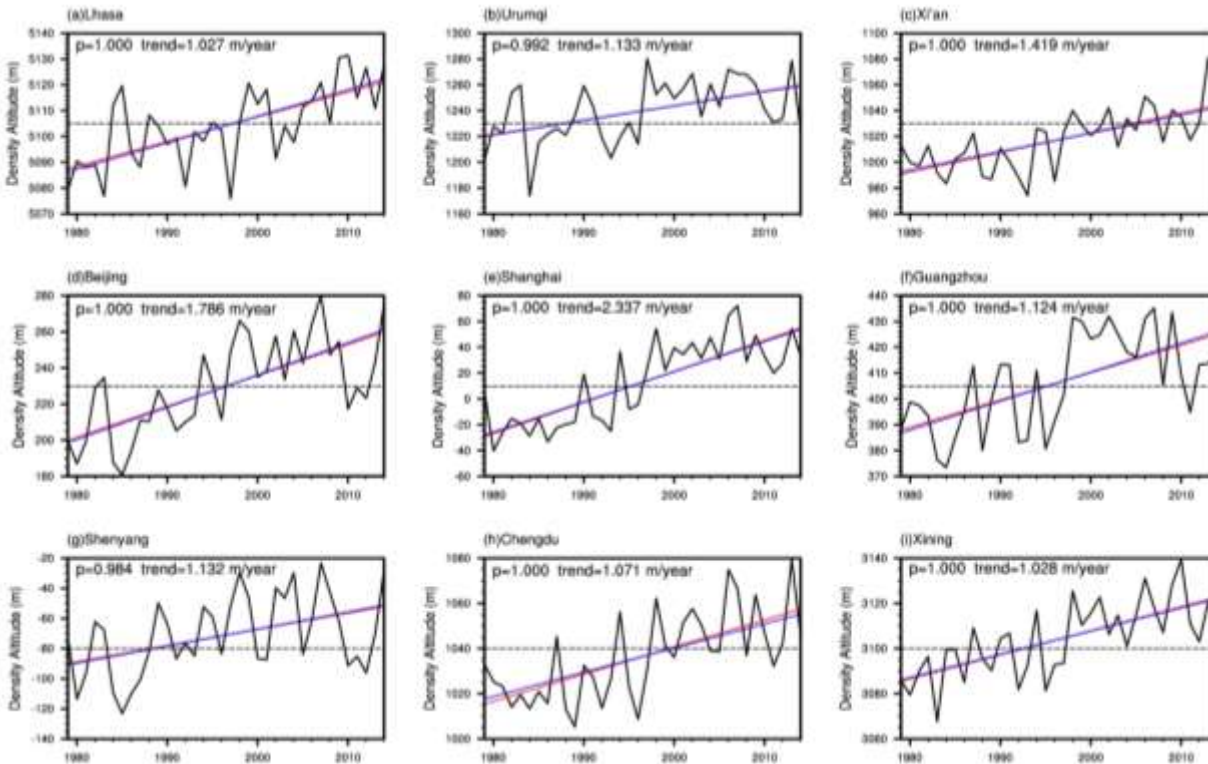


Fig 1: temporal variation of the annual average density altitudes of the nine airports (black line, the black dotted line is the average density altitude of the airport, the red line and blue line are univariate linear

regression and Theil–Sen trend estimation. The p value indicates the significance of the Mann–Kendall trend test).

Different simulation results were obtained when comparing the model simulation data with the ERA-Interim data because of the different model resolutions and model parameterization schemes. In Fig 2, the triangle on the left side of the gridded cell enclosed by each row and column shows the difference between the mean density altitude of the models and the ERA-Interim reanalysis data. The density altitude result in most models was low for Lhasa Airport, where the altitude was the highest, whereas the result was high for Chengdu Airport in the Sichuan Basin, downstream of the Qinghai–Tibet Plateau. The results varied considerably among different models, and the multi-model average fit the measured data well. Each model was able to show the annual variation of density altitude very well, and the correlation coefficients with the reanalysis data were all over 0.9. The maximum density altitude was observed in July and the minimum value was in January (figure not included). In most models, the normalized centered RMS difference was small, as shown by the triangle on the right side of each gridded cell in Fig 2.

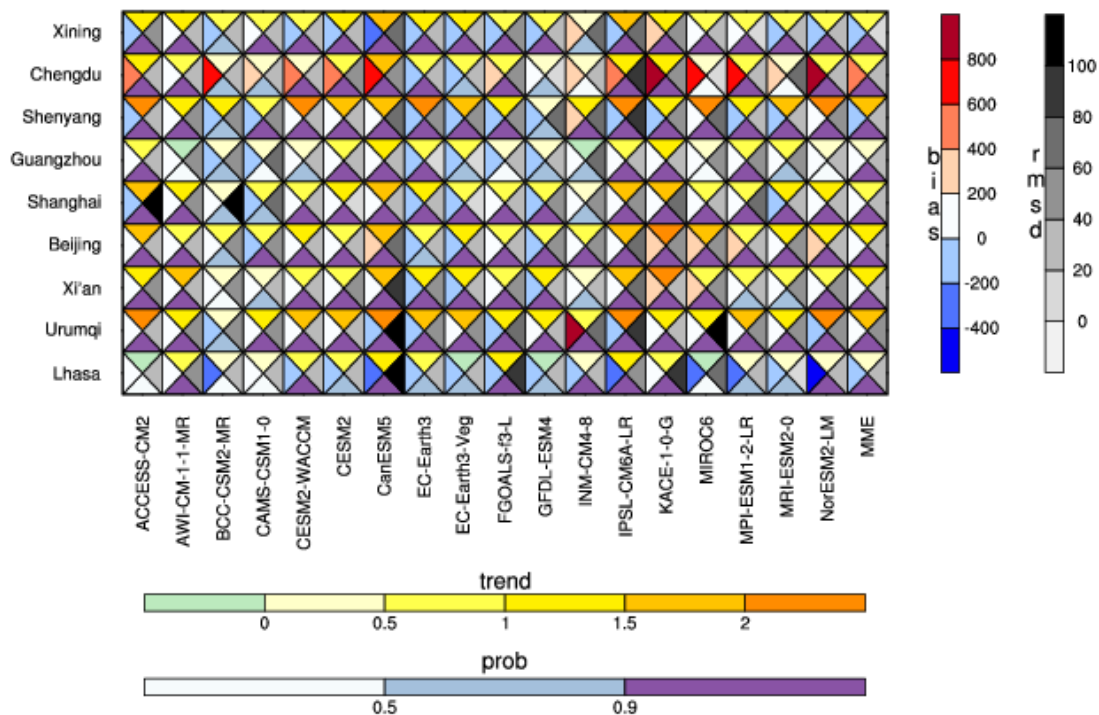


Fig 2: climate statistics of the CMIP6 models. Each box is divided into four parts; the left triangle is the difference between the model average and the reanalysis data, the right triangle is the centered RMS difference in the annual variation between the model and the reanalysis data, and the upper triangle is the Theil–Sen estimation of the annual average density altitude, and the lower triangle is the Mann–Kendall (MK) trend significance test result.

The variation of the annual average density altitude with time is demonstrated in Fig 3. The performance was highly variable among different models. In terms of the correlation coefficients between

the annual average density altitude and time of the reanalysis data for the 18 models, the KACE-1.0-G model had the best performance, for which the correlation coefficients of all nine airports passed the 95% reliability test. The normalized centered RMS difference also performed well. The simulation results of the density altitudes varied among different airports. In general, the statistics of high-altitude airports were highly variable. In addition, it is worth noting that although the results of different models were quite different, the average result including all 18 models was better than that of most individual models.

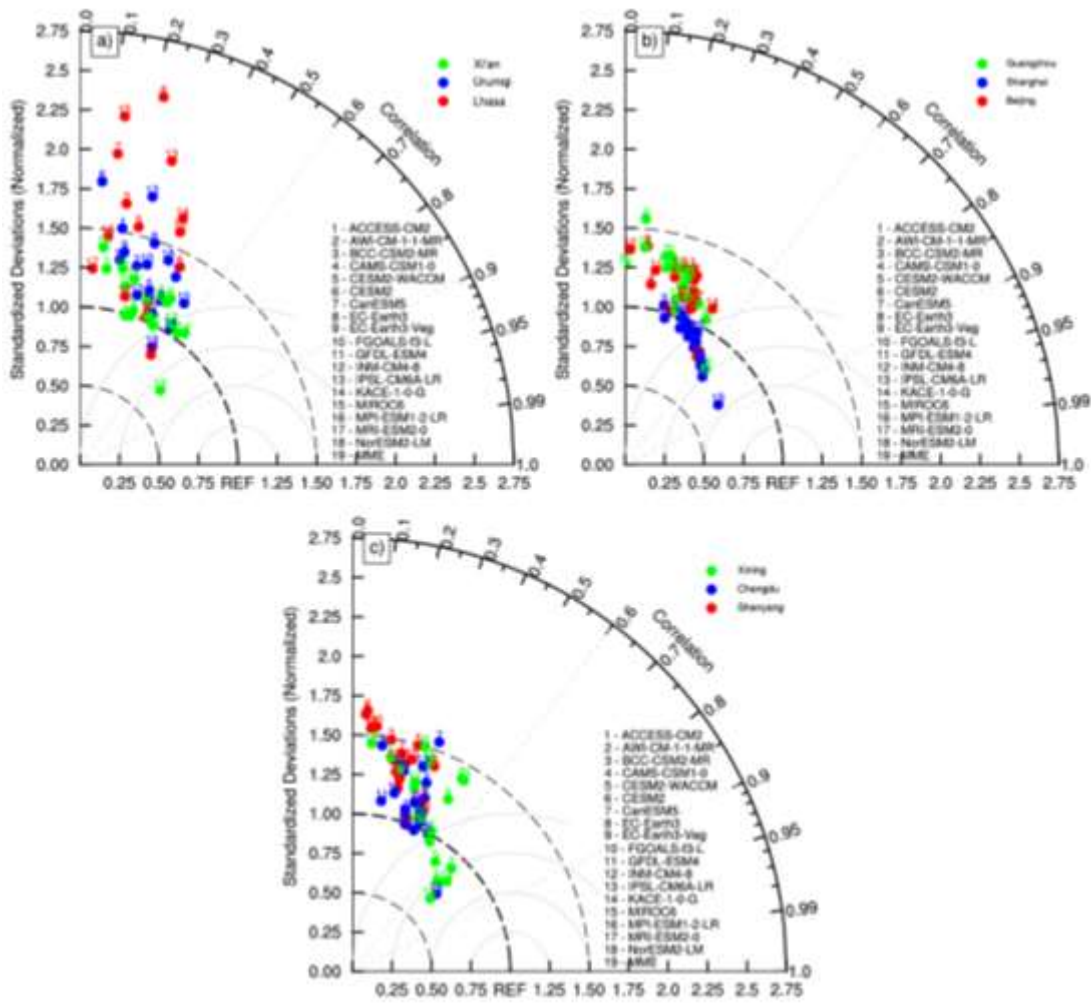


Fig 3: Taylor diagram of annual average density altitudes for the nine airports in the CMIP6 models versus the ERA-Interim reanalysis data. Numbers (1–19) indicate the model number and the multi-model average, the green circle in (a) is the simulation results of the density altitude of Xi'an Airport, the blue and red circles are results of Urumqi Airport and Lhasa Airport, respectively. Those in (b) and (c) are similar to (a).

The simulated variation trend of the annual average density altitude of the 18 models varied among the nine airports. The upper triangle in the gridded cell in Fig 2 represents the trend, and the lower triangle represents the probability. Most of the models showed an increasing trend in the density altitude, however, the simulated trend was smaller than that of the reanalysis data. Moreover, the increasing trends for

Urumqi and Shenyang Airports in most models (including the 18-model average) were larger than those of the reanalysis data. The standard deviation of the trend indicated that the KACE-1.0-G model had the best performance, followed by GFDL-ESM4, BCC-CSM2-MR, and the 18-model average. However, for GFDL-ESM4 and BCC-CSM2-MR, four and nine airports, respectively, showed probabilities of the trend of below 0.9. For KACE-1.0-G and the 18-model average, the probabilities of all nine airports were greater than 0.9. Based on the above analysis, the simulation results of the KACE-1.0-G model was selected to study the density altitude variation of the nine airports.

3.2 Variation Trend of Density Altitude under Different SSP Scenarios

The density altitudes of the nine airports from 2014 to 2100 simulated by KACE-1.0-G all showed an increasing trend under the different SSP scenarios (Fig 4), and passed the Mann–Kendall trend test. Shenyang, Urumqi, and Beijing Airports, located at high latitudes, showed a rapidly increasing density altitude trend under the three scenarios. Under SSP4-8.5, the largest increase was 2.91 m/a. In contrast, Lhasa and Xining Airports, located on the Qinghai–Tibet Plateau, and Chengdu Airport, located in the eastern basin of the plateau, showed slow increasing trends. In SSP4-8.5, the smallest increase was 1.79 m/a. In terms of seasonal variation, contrary to the historical trend, the density altitude of all airports increased fastest in winter.

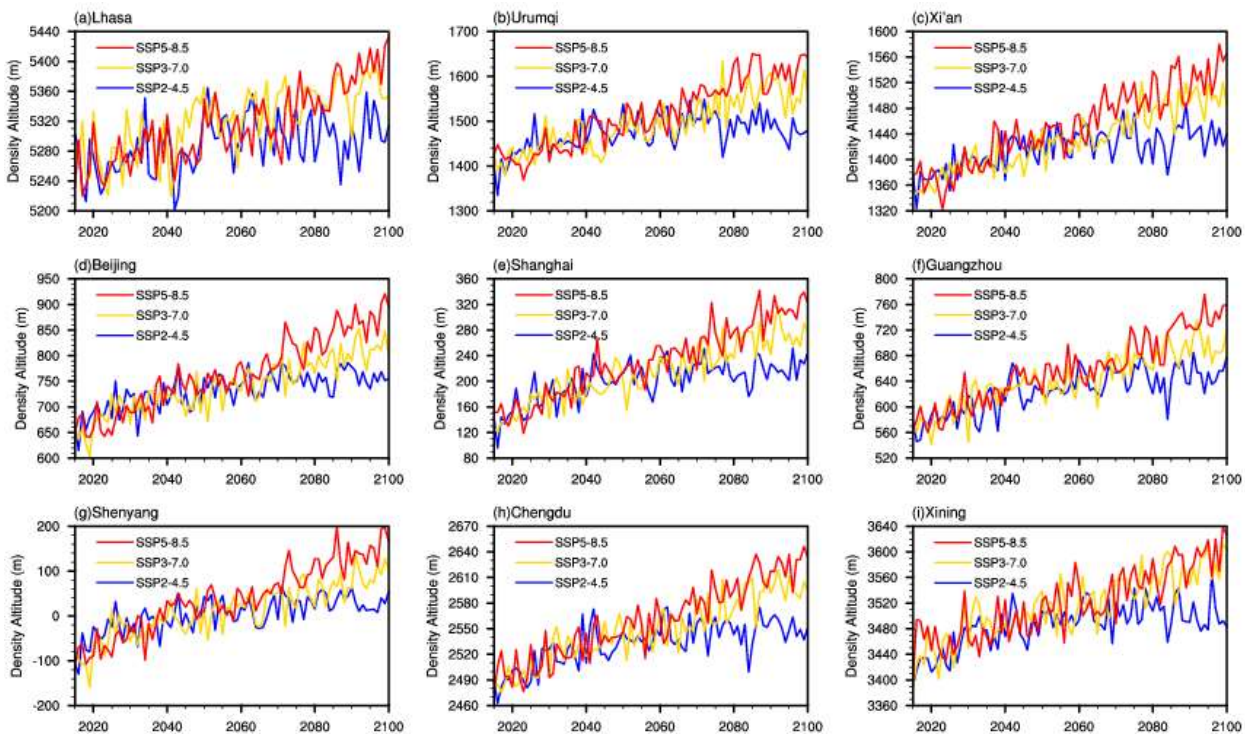


Fig 4: density altitude variations of the nine airports from 2014 to 2100 simulated by the KACE-1.0-G model under different scenarios.

The results of the three scenarios showed that radiative forcing in the early 21st century had little

influence on the magnitude of increase in density altitude. In the mid-to-late 21st century, the warming trends began to show large differences among the three scenarios. In SSP2-4.5, there was very little density altitude variation in the late 21st century. Compared with the reference period from 2005 to 2014, Shenyang and Lhasa Airports had the largest and smallest increase by 2100, respectively. Specifically, the increase was 153.3 m/226.1 m/281.3 m and 15.1 m/76.9 m/106.9 m under the SSP2-4.5, SSP3-7.0, and SSP4-8.5 scenarios, respectively.

IV. CONCLUSION

This study aimed to examine the impact of climate change on the density altitudes of nine selected Chinese airports. We used the near-surface air temperature and surface air pressure data simulated by 18 CMIP6 models to calculate the density altitudes. First, the density altitudes of the nine airports were calculated from the ERA-Interim data from 1979 to 2014, and the results were compared with the results from the 18 models. The KACE-1.0-G model was found to have the best performance, followed by the 18-model average. From 1979 to 2014, all nine airports showed a significant increase in density altitude, with Shanghai Airport and Beijing Airport having the highest increase rates (2.337 m/a and 1.786 m/a). The rates of increase of the two high-altitude airports were very small. When considering the seasonal variation, all airports were found to have the highest increase rate in spring and autumn, except for the two high-altitude airports. The variations in the density altitudes of the nine airports from 2015 to 2100 were then analyzed based on the results of the KACE-1.0-G model under three SSP scenarios. The density altitudes of the nine airports all showed an increasing trend under the different scenarios, and the higher the emission level, the greater the magnitude of the increase. Moreover, the increase in density altitudes at all airports was fastest in the winter. The study is not without limitations. First, we only focused on nine representative airports, and more airports could be included in future work. Second, there are several different ways of calculating the density altitude and the calculation equation used in this study mainly focuses on the influence of air temperature and pressure on the density altitude. In the next step, humidity can be added as an influencing factor.

ACKNOWLEDGEMENTS

This research was supported by Key Program Foundation of Civil Aviation Flight University of China (ZJ2018-05).

REFERENCES

- [1] Penner, J. E., Lister, D., Griggs, D. J., Dokken, D. J., & McFarland, M. (1999). *Aviation and the global atmosphere: a special report of the Intergovernmental Panel on Climate Change*: Cambridge University Press.
- [2] Holmes, C. D., Tang, Q., & Prather, M. J. (2011). Uncertainties in climate assessment for the case of aviation NO_x. *Proceedings of the National Academy of Sciences*, 108 (27), 10997-11002.
- [3] Lee, D. S., Fahey, D., Skowron, A., Allen, M., Burkhardt, U., Chen, Q., Fuglestedt, J. (2021). The contribution of global aviation to anthropogenic climate forcing for 2000 to 2018. *Atmospheric environment*, 244, 117834.
- [4] Lee, D. S., Fahey, D. W., Forster, P. M., Newton, P. J., Wit, R. C., Lim, L. L., Sausen, R. (2009). Aviation and global climate change in the 21st century. *Atmospheric environment*, 43 (22-23), 3520-3537.

- [5] Wuebbles, D., Gupta, M., & Ko, M. (2007). Evaluating the impacts of aviation on climate change. *Eos, Transactions, American Geophysical Union*, 88 (14), 157-160.
- [6] Zhou, C., & Penner, J. E. (2014). Aircraft soot indirect effect on large-scale cirrus clouds: Is the indirect forcing by aircraft soot positive or negative? *Journal of Geophysical Research: Atmospheres*, 119(19), 11,303-311,320.
- [7] Nerem, R. S., Beckley, B. D., Fasullo, J. T., Hamlington, B. D., Masters, D., & Mitchum, G. T. (2018). Climate-change-driven accelerated sea-level rise detected in the altimeter era. *Proc Natl Acad Sci U S A*, 115(9), 2022-2025. doi:10.1073/pnas.1717312115.
- [8] Bengtsson, L., Hodges, K. I., & Roeckner, E. (2006). Storm tracks and climate change. *Journal of Climate*, 19(15), 3518-3543.
- [9] Priestley, M. D., Ackerley, D., Catto, J. L., Hodges, K. I., McDonald, R. E., & Lee, R. W. (2020). An Overview of the Extratropical Storm Tracks in CMIP6 Historical. *Journal of Climate*, 33(15), 6315-6343. doi:10.1175/JCLI-D-19-0928.1
- [10] Zappa, G., Shaffrey, L. C., Hodges, K. I., Sansom, P. G., & Stephenson, D. B. (2013). A multimodel assessment of future projections of North Atlantic and European extratropical cyclones in the CMIP5 climate models. *Journal of Climate*, 26 (16), 5846-5862.
- [11] Coffel, E., & Horton, R. (2015). Climate change and the impact of extreme temperatures on aviation. *Weather, Climate, Society*, 7 (1), 94-102.
- [12] Atrill, J., Sushama, L., & Teufel, B. (2021). Clear-air turbulence in a changing climate and its impact on polar aviation. *Safety in Extreme Environments*, 3 (2), 103-124.
- [13] Storer, L. N., Williams, P. D., & Gill, P. G. (2018). Aviation Turbulence: Dynamics, Forecasting, and Response to Climate Change. *Pure and Applied Geophysics*, 1-15.
- [14] Storer, L. N., Williams, P. D., & Joshi, M. M. (2017). Global response of clear-air turbulence to climate change. *Geophysical Research Letters*, 44 (19), 9976-9984.
- [15] Williams, P. D. (2017). Increased light, moderate, and severe clear-air turbulence in response to climate change. *Advances in Atmospheric Sciences*, 34(5), 576-586.
- [16] Williams, P. D., & Joshi, M. M. (2013). Intensification of winter transatlantic aviation turbulence in response to climate change. *Nature Climate Change*, 3 (7), 644-648.
- [17] Gratton, G., Williams, P. D., Padhra, A., & Rapsomanikis, S. (2022). Reviewing the impacts of climate change on air transport operations. *The Aeronautical Journal*, 126 (1295), 209-221.
- [18] Ren, D., Dickinson, R. E., Fu, R., Bornman, J. F., Guo, W., Yang, S., & Leslie, L. M. (2018). Impacts of climate warming on maximum aviation payloads. *Climate Dynamics*, 1-11.
- [19] Zhou, Y., Zhang, N., Li, C., Liu, Y., & Huang, P. (2018). Decreased takeoff performance of aircraft due to climate change. *Climatic Change*, 151 (3), 463-472.
- [20] Goodman, C. J., & Small Griswold, J. D. (2018). Climate impacts on density altitude and aviation operations. *Journal of Applied Meteorology and Climatology*, 57 (3), 517-523.
- [21] Eyring, V., Bony, S., Meehl, G. A., Senior, C. A., Stevens, B., Stouffer, R. J., & Taylor, K. E. (2016). Overview of the Coupled Model Intercomparison Project Phase 6 (CMIP6) experimental design and organization. *Geoscientific Model Development*, 9 (5), 1937-1958.
- [22] Zhao, Z., Luo, Y., & Huang, J. (2018). The detection of the CMIP5 climate model to see the development of CMIP6 Earth system models. *Climate Change Research*, 14 (6), 643-648.